Research paper

Synthesis, characterization and magnetic study of two new octahedral iron(III) complexes with pendant zwitterionic Schiff bases

Subrata Jana, Anik Bhattacharyya, Biswa Nath Ghosh, Kari Rissanen, Santiago Herrero, Reyes Jiménez-Aparicio, Shouvik Chattopadhyay

PII: S0020-1693(16)30510-2
DOI: http://dx.doi.org/10.1016/j.ica.2016.09.005
Reference: ICA 17250

To appear in: *Inorganica Chimica Acta*

Received Date: 17 March 2016
Revised Date: 31 August 2016
Accepted Date: 5 September 2016

Please cite this article as: S. Jana, A. Bhattacharyya, B. Nath Ghosh, K. Rissanen, S. Herrero, R. Jiménez-Aparicio, S. Chattopadhyay, Synthesis, characterization and magnetic study of two new octahedral iron(III) complexes with pendant zwitterionic Schiff bases, *Inorganica Chimica Acta* (2016), doi: http://dx.doi.org/10.1016/j.ica.2016.09.005

Synthesis, characterization and magnetic study of two new octahedral iron(III) complexes with pendant zwitterionic Schiff bases

Subrata Jana[a], Anik Bhattacharyya[a], Biswa Nath Ghosh[b], Kari Rissanen[b], Santiago Herrero[c], Reyes Jiménez-Aparicio[c], Shouvik Chattopadhyay[a,*]

[a] *Department of Chemistry, Inorganic section, Jadavpur University, Kolkata-700032, India. Mail: shouvik.chem@gmail.com Tel: +91-9007777373*

[b] *Department of Chemistry, Nanoscience Center, University of Jyväskylä, P.O. Box 35, 40014 Jyväskylä, Finland.*

[c] *Departamento de Química Inorgánica, Facultad de Ciencias Químicas, Universidad Complutense de Madrid, Madrid, Spain.*

Abstract

Two Schiff bases, HL^1 [2-((3-(dimethylamino)propylimino)methyl)-5-bromophenol] and HL^2 [2-((2-(diethylamino)ethylimino)methyl)-6-methoxyphenol], have been employed to prepare two new octahedral iron(III) complexes, $[Fe(HL^1)_2(N_3)_2]ClO_4{\cdot}2H_2O$ (**1**) and $[Fe(HL^2)_2(NCS)_2]ClO_4{\cdot}H_2O$ (**2**). Both complexes are characterized by spectral and elemental analyses. Single crystal X-ray diffraction studies confirm their structures. In both complexes, Schiff bases are trapped in their zwitterionic forms and coordinated to iron(III) only through the imine nitrogen and phenoxo oxygen, i.e., they behave as bi-dentate ligands, keeping the remaining potential donor sites pendant. The measurement of χ_M vs. T for both complexes shows

a continuous increase in susceptibility as the temperature decreases. The $\chi_M \cdot T$ values from 300 to 2 K and the shape of these curves for both complexes discard the existence of a high-spin/low-spin transition. The decrease in $\chi_M \cdot T$ of **1** with temperature is more pronounced than that expected for a complex with a small zero-field splitting. The magnetic behavior of **1** is explained by proposing the existence of a physical mixture of $S = 5/2$ and $S = 1/2$ spins and the presence of zero-field splitting in the $S = 5/2$ species.

Keywords: Iron(III); Crystal Structure; Zwiterionic; Pendant; Variable temperature magnetic susceptibility

1. Introduction

The rational design and construction of iron(III) Schiff base complexes have attracted extensive interest due to their structural diversity and potential applications in molecular magnetism as an important class of spin crossover (SCO) systems because of the possibility of the co-existence of two different magnetic states under the same conditions [1,2]. The phenomenon of spin cross-over is induced by external perturbations, such as pH, temperature, pressure, light irradiation, etc. [3-7]. The iron(III) sites in some heme proteins also reported to exhibit SCO behavior, which plays a key role in their biological functions [8-10].

Several iron(III) complexes of various geometry have been prepared using different chelating ligands [11-13], of which Schiff bases are special choices for the easy routes of their synthesis, the wide range of their stability and their very good complexing ability [14-19]. Among them, H_2salen type tetradentate Schiff bases, prepared by 1:2 condensations of any diamines with salicylaldehyde derivatives, are, of course, receiving the most attention [20-24]. In the octahedral iron(III)-salen complexes with other co-ligands, two different arrangements of

four donor atoms around the iron(III) is found; one in which the donors occupy the four equatorial positions [25-29] the other in which one oxygen is displaced from the equatorial plane, occupying an axial position of the coordination polyhedron [30-33]. Variable temperature magnetic susceptibility measurements identified the presence of SCO points in some of the complexes [34, 35]. On the other hand, N_2O donor Schiff bases, prepared by 1:1 condensation of any N-substituted diamine with suitable salicylaldehyde derivative have also been used to prepare various iron(III) complexes [36-44] of which mononuclear octahedral bis–ligand complexes constitute a unique class, as most of them show SCO behavior [36-39].

In the present work, we have used two potential tridentate Schiff bases to synthesize two similar mononuclear octahedral iron(III) complexes, in which the zwiterionic forms of two Schiff bases have been trapped. Structures of both complexes have been confirmed by single crystal X-ray crystallography. Both Schiff bases are behaving as bidentate ligands keeping the remaining donor sites pendant. Variable temperature magnetic susceptibilities of both complexes have also been measured. Herein, we would like to report the synthesis, characterization and magnetic properties of two new octahedral iron(III) complexes, $[Fe(HL^1)_2(N_3)_2]ClO_4{\cdot}2H_2O$ (**1**) and $[Fe(HL^2)_2(NCS)_2]ClO_4{\cdot}H_2O$ (**2**), with two pendant Schiff bases, HL^1 [= 2-((3-(dimethylamino)propylimino)methyl)-5-bromophenol] and HL^2 [= 2-((2-(diethylamino)ethylimino)methyl)-6-methoxyphenol].

2. Experimental Section

2.1. Materials and physical measurements

All chemicals were of reagent grade and used as purchased from Sigma-Aldrich without further purification.

Elemental analyses (carbon, hydrogen and nitrogen) were carried out using a PerkinElmer 2400 II elemental analyzer. IR spectra in KBr (4000–400 cm^{-1}) were recorded using a PerkinElmer Spectrum Two Fourier transform infrared (FTIR) spectrophotometer. The UV−visible spectra were recorded on a PerkinElmer lambda 35 spectrophotometer at 298 K in acetonitrile.

The variable-temperature magnetization data were acquired on polycrystalline samples obtained from crushed crystals with a Quantum Design MPMSXL SQUID (Superconducting Quantum Interference Device) magnetometer over a temperature range of 2 to 300 K at the constant field of 1 T and 0.1 T. Each raw data set was corrected for the diamagnetic contribution of both the sample holder and the complex to the susceptibility. The molar diamagnetic corrections were calculated on the basis of Pascal constants [45-48]. Magnetization measurements at 2 K from -5 T to 5 T were carried out to check the existence of cooperative phenomena.

CAUTION!!! Metal perchlorates containing azide and/or organic ligands are potentially explosive. Although no problem was encountered in the present study, small amounts of the materials should be prepared and must be handled with great care.

2.2. Synthesis

2.2.1. Synthesis of the ligands, HL^1 and HL^2

The Schiff base ligand, HL^1 was synthesized by refluxing N,N-dimethyl-1,3-diaminopropane (1 mmol, 0.13 mL) with 5-bromosalicylaldehyde (1 mmol, 0.201 g) in methanol for ca. 1 h. The ligand was not isolated and used directly for the synthesis of the complex **1**.

The Schiff base ligand, HL^2 was synthesized in a very similar way by refluxing N,N-diethyl-1,2-diaminoethane (1 mmol, 0.14 mL) with 3-methoxysalicylaldehyde (1 mmol, 0.152 g) in methanol for ca. 1 h. The ligand was also not isolated and used directly for the synthesis of the complex **2**.

*2.2.2. Synthesis of $[Fe(HL^1)_2(N_3)_2]ClO_4{\cdot}2H_2O$ (**1**)*

A methanol solution (20 ml) of iron(III) perchlorate (1 mmol, 0.354 g) was added to the methanol solution of the ligand HL^1 (2 mmol) and refluxed for 1 h. A (2:1) methanol/water solution (5 ml) of sodium azide (2 mmol, 0.130 g) was then added to it and refluxed further for ca. 1 h. A black precipitate was separated out and collected by filtration and re-crystallized from acetonitrile/dichloromethane (1:1) solution. Diffraction quality single crystals were isolated from this re-crystallized product.

Yield: 0.435 g (51%). Anal. Calc. for $C_{24}H_{38}Br_2ClFeN_{10}O_8$ (FW 845.73): C, 34.08; H, 4.53; N, 16.56; Found: C, 34.1; H, 4.6; N, 16.7; % IR (KBr, cm^{-1}): 1624 ($\nu_{C=N}$), 2045 (ν_{N3}), 1094 (ν_{ClO4}), 3045 (ν_{C-H}), 3433 (ν_{O-H}), UV–Vis, λ_{max} (nm) [ε_{max}/L mol^{-1} cm^{-1}] (CH_3CN), 220 (3.3×10^3), 240 (2.1×10^3), 324 (8.1×10^2), 505 (3.1×10^2).

*2.2.3. Synthesis of $[Fe(HL^2)_2(NCS)_2]ClO_4{\cdot}H_2O$ (**2**)*

Complex **2** was prepared in a similar method to that of complex **1**, except that sodium thiocyante (2 mmol, 0.162 g) and ligand HL^2 (2 mmol) were added instead of sodium azide and ligand HL^1. It was re-crystallized from acetonitrile solution. Diffraction quality single crystals were isolated from this re-crystallized product.

Yield: 0.420 g (53%). Anal. Calc. for $C_{30}H_{44}ClFeN_6O_9S_2$ (FW 788.13): C, 45.72; H, 5.63; N, 10.66; Found: C, 45.8; H, 5.7; N, 10.7;% IR (KBr, cm^{-1}): 1616 ($\nu_{C=N}$), 2061 (ν_{SCN}), 1084 (ν_{ClO4}), 3055 (ν_{C-H}), 3439 (ν_{O-H}), UV–Vis, λ_{max} (nm) [ε_{max}/L mol^{-1} cm^{-1}] (CH_3CN), 212 (3.0×10^3), 265 (1.3×10^3), 342 (4.1×10^2), 437(3.3×10^2).

2.3. X-ray crystallography

The structural analysis of complex **1** was performed on an Agilent SuperNova diffractometer with Atlas detector using mirror-monochromatized Mo-*K*α (λ = 0.71073 Å) radiation at 173 K. *CrysAlis*^{PRO} program was used for data collection and processing [49]. The intensities were corrected for absorption using the built-in absorption correction method [50]. The structure was solved with the program *Superflip* [51] and refined by full-matrix least squares on F^2 using the *WinGX* [52] software equipped with SHELXL-2014 [53]. The perchlorate anion was found to be disordered over two positions. The oxygen atoms of perchlorate anion were kept as isotropic model. All other non-hydrogen atoms were refined with anisotropic thermal parameters. All hydrogen atoms were calculated to their optimal positions and treated as riding atoms using isotropic displacement parameters 1.2 larger than the respective host atoms.

Single crystals of the complex **2**, having suitable dimensions, were used for data collection using a 'Bruker SMART APEX II' diffractometer equipped with graphite-monochromated Mo-Kα radiation (λ = 0.71073 Å) at 273 K. The molecular structure was solved by direct methods and refinement by full-matrix least squares on F^2 using the SHELX-2014 package [53]. Non-hydrogen atoms were refined with anisotropic thermal parameters. Hydrogen atoms were placed in their geometrically idealized positions and constrained to ride on their parent atoms. Multi-scan empirical absorption corrections were applied to the data using the

program SADABS [54]. A summary of the crystallographic data are given in Table 1. CCDC reference numbers are 1406301 and 1406302 for **1** and **2** respectively.

2.4. Hirshfeld surface analysis

Hirshfeld surfaces [55-57] and the associated two dimensional fingerprint [58-60] plots were calculated using Crystal Explorer [61], with bond lengths to hydrogen atoms set to standard values [62]. For each point on the Hirshfeld isosurface, two distances d_e, the distance from the point to the nearest nucleus external to the surface and d_i, the distance to the nearest nucleus internal to the surface, are defined. The normalized contact distance (d_{norm}) based on d_e and d_i is given by

$$d_{norm} = \frac{(d_i - r_i^{vdw})}{r_i^{vwd}} + \frac{(d_e - r_e^{vdw})}{r_e^{vwd}}$$

where r_i^{vdW} and r_e^{vdW} are the van der Waals radii of the atoms. The value of d_{norm} is negative or positive depending on whether the intermolecular contacts are shorter or longer than the van der Waals separations. The parameter d_{norm} displays a surface with a red–white–blue colour scheme, where bright red spots highlight shorter contacts, white areas represent contacts around the van der Waals separation, and blue regions are devoid of close contacts. For a given crystal structure and set of spherical atomic electron densities, the Hirshfeld surface is unique [63] and provides additional insight into intermolecular interactions in molecular crystals.

3. Results and discussion

3.1. Synthesis

In the present work, we have used two Schiff bases (HL^1 and HL^2) to synthesize two iron(III) complexes. HL^1 was prepared by the condensation of N,N-dimethyl-1,3-diaminopropane with 5-bromosalicylaldehyde following literature method [43]. HL^2 was synthesized in a very similar way using N,N-diethyl-1,2-diaminoethane and 3-methoxysalicylaldehyde. Addition of iron(III) perchlorate and sodium azide in the methanol solution of the ligand HL^1 produces complex **1**. On the other hand, addition of iron(III) perchlorate and sodium thiocyante in the methanol solution of the ligand HL^2 results in the formation of complex **2**. The schematic representations of structures of both ligands (zwitterionic and non-zwitterionic forms) are shown in Scheme 1 while that of both complexes are shown in Scheme 2. Probably the use of perchlorate salt increases the acidity of the medium and favours the non-deprotonation of the Schiff bases (zwittereionic form) thereby forcing them to act as bidentate ligands in the iron(III) complexes.

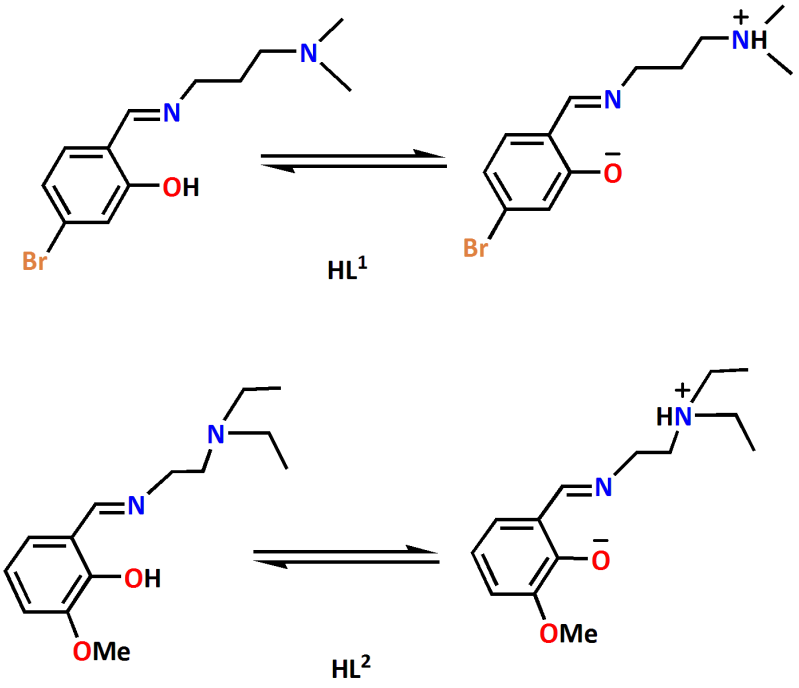

Scheme 1: Sketch of the ligands (zwitterionic and non-zwitterionic forms) used in this work.

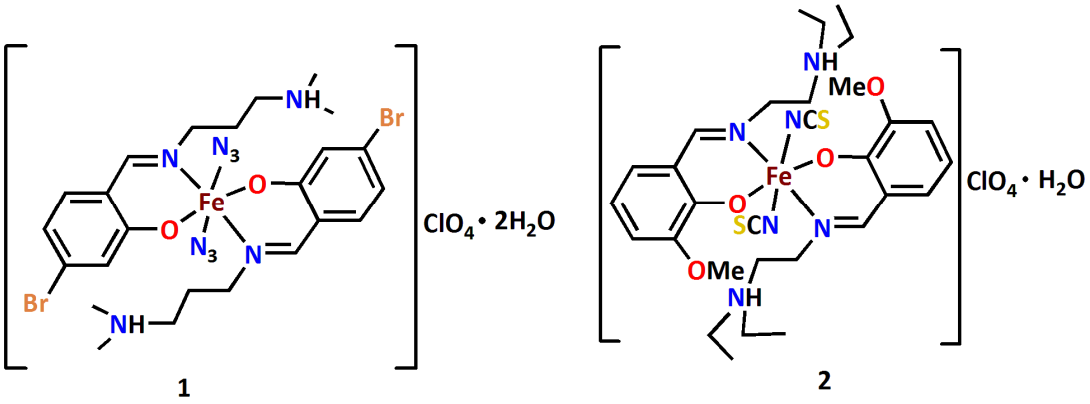

Scheme 2: Sketch of the complexes used in this work.

3.2. Description of structures

*3.2.1.[Fe(HL^1)$_2$(N$_3$)$_2$]ClO$_4$·2H$_2$O (**1**)*

Complex **1** crystallizes in the monoclinic space group *C2/c*. A perspective view of complex **1** with selective atom-numbering scheme is shown in Figure 1. The asymmetric unit contains one discrete centrosymmetric mononuclear iron(III) center [Fe(HL^1)$_2$(N$_3$)$_2$], one perchlorate ion and two solvent water molecules. The Fe(1) center is octahedrally coordinated by two phenoxo oxygen atoms, O(1) and O(1)* (* = 1/2-x,3/2-y,-z) and two imine nitrogen atoms, N(1) and N(1)* of two Schiff base ligands (HL^1) and by two nitrogen atoms N(3) and N(3)* from two azide groups. The Fe(1)-O(1), Fe(1)-N(1) and Fe(1)-N(3) bond lengths are 1.933(3), 2.135(4) and 2.085(4) Å, respectively, which are close to those in other related iron(III) complexes [43]. Selected bond distances and bond angles of complex **1** are given in Table 2. The azide group is almost linear [N(3)-N(4)-N(5) = 178.6(5)°].

The hydrogen atom, H(2A), attached to amine nitrogen atom, N(2), is involved in hydrogen bonding interaction with the symmetry related (x,1-y,1/2+z) oxygen atom, O(2)$^\$$ of

water molecule. Similarly, hydrogen atoms, H(2B) and H(2C), attached to the oxygen atom, O(2), are involved in hydrogen bonding interactions with the symmetry related (1/2-x,3/2-y,-z) phenoxo oxygen atom, $O(1)^{*}$ and azide nitrogen atom, $N(3)^{*}$, respectively. Complex **1** forms a two dimensional supramolecular architecture via hydrogen bonding interactions (Figure 2). Details of the hydrogen bonding interaction are given in Table 3. On the other hand, the hydrogen atom, H(10B), attached to C(10), is involved in intermolecular C–H···π interaction with the symmetry related (1/2-x,1/2+y,1/2-z) phenyl ring C(1)–C(2)–C(3)–C(4)–C(5)–C(6). Similarly, hydrogen atom, H(12A), attached to C(12), is involved in intermolecular C–H···π interaction with the symmetry related (1/2-x,-1/2+y,1/2-z) phenyl ring C(1)–C(2)–C(3)–C(4)–C(5)–C(6) to form a two dimensional sheet, as shown in Figure 3. Geometric features of the C–H···π interactions are given in Table 4. One interesting observation in the crystal structure of complex **1** is that the bromine atom of the Schiff base shows close contact (3.619(1) Å) with a symmetry related (-x,y,1/2-z) bromine atom from a nearest neighbor. The distance is less than the sum (3.8 Å) of their van der Wall radii. Although the Br···Br interaction is not very common, examples of this type of interactions could be found in literature [64]. The Br···Br interaction in complex **1** creates a one-dimensional chain along crystallographic a axis, as shown in Figure 4.

*3.2.2. $[Fe(HL^2)_2(NCS)_2]ClO_4{\cdot}H_2O$ (**2**)*

Complex **2** crystallizes in the orthorhombic space group *Pnma*. A perspective view of complex **2** with selective atom numbering scheme is shown in Figure 5. The asymmetric unit contains one discrete centrosymmetric mononuclear iron(III) center $[Fe(HL^2)_2(NCS)_2]$, one perchlorate ion and one solvent water molecule. The Fe(1) centre is octahedrally coordinate by two phenoxo oxygen atoms, O(1) and $O(1)^{\#}$ ($^{\#}$ = 1-x,1-y,1-z) and two imine nitrogen atoms, N(1) and $N(1)^{\#}$ of two Schiff base ligands (HL^1) and by two nitrogen atoms N(3) and $N(3)^{\#}$ from two

thiocyanate groups. The Fe(1)-O(1), Fe(1)-N(1) and Fe(1)-N(3) bond lengths are 1.948(3), 2.115(3) and 2.082(4) Å, respectively, which are close to those in other related iron(III) complexes [43]. The thiocyanate group is almost linear [N(3)-C(1)-S(1) = 178.0(4)°].Selected bond distances and bond angles of complex **2** are given in Table 2. The hydrogen atom H(2A), attached to amine nitrogen atom N(2) is involved in hydrogen bonding interaction with the symmetry related (1-x,1-y,1-z) methoxy oxygen atom O(2)$^{\#}$ (Figure 5). Details of the hydrogen bonding interaction are given in Table 3.

The hydrogen atom, H(15B), attached to C(15), is involved in intermolecular C–H···π interaction with the symmetry related (1/2+x,y,1/2-z) phenyl ring C(1)–C(2)–C(3)–C(4)–C(5)–C(6) to form a two dimensional sheet, as shown in Figure 6. Geometric features of the C–H···π interactions are given in Table 4.

3.3. IR and electronic spectra

In the IR spectra of both complexes, distinct bands due to azomethine (C=N) groups are routinely observed around 1615 cm^{-1} [65]. Complexes **1** and **2** show strong bands respectively at 2045 and 2061 cm^{-1} due to the presence of monodentate azide and thiocyanate [65]. Both complexes show broad bands around 1090 cm^{-1} due to the presence of perchlorate anion [65]. The broad bands around 3400 cm^{-1} indicate the presence of solvent water molecules in both complexes [66].

Electronic spectra of both complexes were recorded in acetonitrile in the range of 200–800 nm. The intense absorption bands at short wavelengths (220 nm for **1** and 212 nm for **2**), are attributed to π–π* transitions of the ligand and the absorption band around 250 nm (240 nm for **1** and 265 nm for **2**), may be assigned as n–π* transitions [43]. The spectra show a band in the visible region (505 nm for **1** and 437 nm for **2**) assigned to azide/thiocyanate-to-iron(III) charge

transfer (CT). Moreover a moderately strong band (324 nm for **1** and 342 nm for **2**) is a superposition of the amino-to-iron(III) and oxygen to iron(III) CT band [67,68].

3.4. Magnetic properties

Magnetic susceptibilities of complexes **1** and **2** have been measured over the temperature range 2-300K both at 1 T and at 0.1 T. The differences found between the measurements with both fields are not significant. The magnetic data of both complexes are similar. The plot of the magnetic susceptibility vs. temperature of complexes **1** and **2** shows a continuous increase in susceptibility as the temperature decreases, typical of paramagnetic complexes (Figures 7 and 8). The magnetic moment at room temperature of **1** and **2** are 5.28 and 5.70 μ_B, respectively. The magnetic moment of **1** is lower than the expected (5.92 μ_B) for a magnetically isolated high-spin iron(III) ion (S = 5/2) whereas the magnetic moment of **2** is closer to the theoretical value. The representation of $\chi_M \cdot T$ versus temperature for **1** shows an almost constant value of 3.48 emu·mol^{-1}·K from 300 K until at around 70 K. From this point, the $\chi_M \cdot T$ values slowly decrease until at about 25 K and, afterwards, a deeply decrease until 1.57 emu·mol^{-1}·K is observed (Figure 8). This value is higher than the expected (0.375 emu·mol^{-1}·K) for an isolated low-spin iron(III) ion (S = 1/2). For **2** the $\chi_M \cdot T$ value of 4.06 emu·mol^{-1}·K, at room temperature, remains almost constant until at around 11 K and then abruptly decreases to a minimum value of 2.59 emu mol^{-1} K (Figure 7). The representation of magnetization measurements at 2 K (Figure S1 and S2 for **1** and **2**, respectively, supplementary material) carried out between -5 and 5 T show no hysteresis loop. The $\chi_M \cdot T$ values from 300 to 2 K and the shape of these curves for both complexes discard the existence of a high-spin/low-spin transition in spite of the spin crossover phenomenon is very usual in iron(III) complexes [69-71]. However, the decrease at very low temperature can be attributed to an anisotropic distortion of the iron(III) environment, which results in a small zero-

field splitting of the ground state [72]. The plot of $1/\chi_M$ versus T for **1** and **2** complexes (Figure S3 and S4, supplementary material) reveals that the complexes exhibit, basically, a Curie behavior, which confirms the absence of significant cooperative phenomena in both complexes. The magnetic moment value of **2** at room temperature is in the experimental range for d^5 high spin complexes [73]. Thus, the magnetic data can be fitted using the equation 1, which considers the magnetic susceptibility of a high-spin iron(III) (S = 5/2) ion in an axially distorted octahedral environment.

$$\chi = \frac{Ng^2\beta^2}{12kT}\left[\frac{19+16/x+(9-11/x)e^{-2x}+(25-5/x)e^{-6x}}{1+e^{-2x}+e^{-6x}}\right] \qquad (1)$$

In Eq.1, x = D/kT, and D is the zero-field splitting parameter of the S =5/2 spin. The terms N, β, k, and T have the usual meanings. The best fit (Figure 7) was obtained with the following parameters: g = 1.93, D = 3.34 cm^{-1} and σ^2 = 3.0 10^{-3}. The D values are of the same order of other high-spin iron(III) complexes [74,75] and the agreement factor defined as: $\Sigma_i[(\chi_M T)_{obs}(i)-(\chi_M T)_{calc}(i)]^2/\Sigma_i[(\chi_M T)_{obs}(i)]^2$ indicates a good agreement between experimental and calculated data.

However, as stated above, the magnetic moment at room temperature for **1** is lower than the expected for a S = 5/2 spin complex. In addition, the decrease of $\chi_M \cdot T$ with temperature is more pronounced than the expected for a complex with a small zero-field splitting. The existence of an intermediate spin state, or a quantum spin admixture between high and intermediate spin states, can be discarded taking into account the stereochemical environment of the iron centre [76]. The magnetic behavior of **1** might be explained by the existence of a physical mixture of S = 5/2 and S = 1/2 spins and the presence of zero-field splitting in the S = 5/2 species (Eq. 2).

$$\chi = \frac{N g_1^2 \beta^2}{12kT}\left[\frac{19+16/x+(9-11/x)e^{-2x}+(25-5/x)e^{-6x}}{1+e^{-2x}+e^{-6x}}\right](1-\rho)+\frac{N g_2^2 \beta^2}{4kT}\rho \qquad (2)$$

The first term corresponds to the contribution to the magnetic susceptibility of a high-spin iron(III) (S = 5/2) ion in an axially distorted octahedral environment; the second term corresponds to a low-spin iron(III) complex (S = 1/2) and ρ represents the fraction of the low-spin complex in the mixture. To avoid over-parametrization g_1 and g_2 were fixed (g_1= g_2= 2). The parameters obtained in the best fit were D = 9.25 cm^{-1}, ρ = 23 %, and σ^2 = 3.0 10^{-3} (Figure 8). The application of this model to the **2** data gave the following parameters: D = 3.36 cm^{-1}, ρ = 7 %, and σ^2 = 3.0 10^{-3}. The D values are of the same order of other high-spin iron(III) complexes [73,74]. As a consequence, these fits are in accordance with a physical mixture for **1** of 77% of the high-spin complex and a 23% of the low-spin species, and for **2** of 93% of the high-spin complex and a 7% of the low-spin species. This model explains well the magnetic data of **1**. However, the coexistence of two magnetic species with the same nature but different spin configuration along the whole range of temperature and the lack of spin transition seems to be unlikely, unless there is a mechanism that prevents the transition to occur. A possible explanation could be the coexistence of two complexes in the bulk material: one of them containing the Schiff base coordinated in the zwitterionic form (about 77%, high spin) and the other having the Schiff base in the (deprotonated) non-zwittwerionic form (about 23%, low spin). Although a mixture of both non-zwitterionic and zwitterionic forms has been found spectroscopically for sodiated arginine [77], the presence of both forms in the solid state is difficult to demonstrate by X-ray diffraction. However, it has been demonstrated that even two identical species can crystallized with two different spin configurations due to residual interactions in the solid state [78].

3.5. Hirshfeld surface analysis

The Hirshfeld surfaces mapped with d_{norm} for the complexes **1** and **2** are illustrated in Figures 9 and 10, respectively. The dominant interactions between N···H, O···H and C···H atoms in all the complexes can be seen in the Hirshfeld surface as the bright red areas. Other visible spots in the Hirshfeld surfaces correspond to H···H contacts. The small extent of area and light colour on the surface indicates weaker and longer contact other than hydrogen bonds. 2D fingerprint plots complement these surfaces, quantitatively summarizing the nature and type of intermolecular contacts experienced by the molecules in the crystal. The O···H/H···O intermolecular interactions appear as distinct spikes in the 2D fingerprint plots of both complexes. The fingerprint plots can be decomposed to highlight particular atoms pair close contacts [79]. This decomposition enables separation of contributions from different interaction types, which overlap in the full fingerprint. The amount of O···H/H···O interactions comprises 22.1% and 25.2% of the Hirshfeld surfaces for each molecule of complex **1** and **2** respectively.

4. Conclusion

This paper describes the synthesis and X-ray structure of two new octahedral iron(III) complexes containing zwitterionic Schiff bases and pseudo-halides. Both Schiff bases do not use all of their potential donor atoms and therefore do behave as pendant ligands. The magnetic moment value of **2** at room temperature is in the experimental range for d^5 high spin complexes. The variable temperature magnetic susceptibility data of **2** was fitted to the appropriate equation and the best fit zero-field splitting parameter is of the same order of other high-spin iron(III) complexes. However, the magnetic moment at room temperature for **1** is lower than the expected for a high-spin iron(III) complex. The decrease of $\chi_M T$ with temperature is also more pronounced than that expected for a complex with a small zero-field splitting.

Acknowledgements

This work was supported by CSIR, India (Fellowship for Subrata Jana, Sanction No. 09/096(0659)/2010-EMR-I, dated 18.1.11). A.B. thanks the UGC, India, for awarding a Senior Research Fellowship.

References

[1] P. Gütlich, H. A. Goodwin, ed., Top. Curr.Chem, (2004) 233–235.

[2]R.Herchel, Z.Trávníček,Dalton Trans., 42, (2013) 16279-16288.

[3] H. A. Goodwin, Coord. Chem. Rev. 18 (1976) 293-325.

[4] E. König, Prog. Inorg.Chem. 35 (1987) 527-622.

[5] P. Gütlich, Y. Garcia, T. Woike, Coord. Chem. Rev. 219–221 (2001) 839-879.

[6] P. Gütlich, A. Hauser, H. Spiering, Angew. Chem. Int. Ed. 33(1994) 2024-2054.

[7] P. Gütlich, Y. Garcia, H.A. Goodwin, Chem. Soc. Rev. 29 (2000)419-427.

[8] A. H. Ewald, R. L. Martin, I. G. Ross, A. H. White, Proc. Roy. Soc. A 280(1984) 235-257.

[9] G. Harris, Theor. Chim.Acta 5 (1966) 379-397.

[10] M. Zerner, M.Gouterman, H. Kobayashi, Theor. Chim.Acta 6 (1966) 363-400.

[11] M.Poureskandari, E.Safaei, S. M. Sajjadi, T.Karimpour, Z.Jaglicic, Y.-Ill Lee, J. Mol. Struct. 1094 (2015) 130-136.

[12]T.Huxel, M.Skaisgirski, J.Klingele, Polyhedron 93 (2015) 28-36.

[13]K. Santo, M.Hirotsu, I. Kinoshita, Dalton Trans., 44 (2015) 4155-2166.

[14]R. Ziessel, Coord. Chem. Rev. 216 (2001) 195-223.

[15] P.G. Cozzi, Chem. Soc. Rev. 33 (2004) 410-421.

[16] K.C. Gupta, A.K. Sutar, Coord. Chem. Rev. 252 (2008) 1420-1450.

[17] J.P. Costes, S. Shova, W. Wernsdorfer, Dalton Trans. (2008) 1843-1849.

[18] X.G. Ran, L.Y. Wang, Y.C. Lin, J. Hao, D.R. Cao, Appl. Organomet. Chem. 24 (2010) 741-747.

[19] M. Orio, O. Jarjayes, H. Kanso, C. Philouze, F. Neese, F. Thomas, Angew. Chem.Int. Ed. 49 (2010) 4989-4992.

[20] F. Y. Wei, P. H. Wen, Russian J. Coord. Chem. 40 (2014) 289-296.

[21] M. Sutradhar, T. R. Barman, M. G. B. Drew, E. Rentschler, J. Mol. Struct. 1041 (2013) 44-49.

[22] J. S. Pap, A. Matuz, G. Barath, B. Kripli, M. Giorgi, G. Speier, J. Kaizer, J. Inorg. Biochem. 108 (2012) 15-21.

[23] A. J. Clarke, N. Yamamoto, P. Jensen, T. W. Hambley, Dalton Trans. (2009) 10787-10798.

[24] G. Barath, J. Kaizer, G. Speier, L. Parkanyi, E. Kuzmann, A. Vertes, Chem. Commun. (2009) 3630-3632.

[25] Y. Nishida, K. Kino, S. Kida, J. Chem. Soc.Dalton Trans. (1987) 1157-1161.

[26] S. Majumder, S. Dutta, L. M. Carrella, E. Rentschler, S. Mohanta, J. Mol. Struct. 1006 (2011) 216-222.

[27] W. Chiang, D. Vanengen,M. E. Thompson, Polyhedron 15 (1996) 2369-2376.

[28] M. Sarwar, A. M. Madalan, F.Lloret, M. Julve, M. Andruh, Polyhedron 30 (2011) 2414-2420.

[29] H. -L. Shyu, H. -H. Wei, G. -H. Lee, Y. Wang, J. Chem. Soc. Dalton Trans. (2000) 915-918.

[30]J. C. Fanning, X. Wang, A. E. Koziol, G. J. Palenik, Inorg. Chim.Acta 232 (1995) 199-201.

[31] T. W. Failes, T. W. Hambley, J. Inorg. Biochem. 101 (2007) 396-403.

[32] D. J. Darensbourg, C. G. Ortiz, D. R. Billodeaux, Inorg. Chim. Acta, 357 (2004) 2143-2149.

[33] J. S. Pap, A. Matuz, G. Barath, B. Kripli, M. Giorgi, G. Speier, J. Kaizer, J. Inorg. Biochem. 108 (2012) 15-21.

[34]T. M. Ross, S. M. Neville, D. S. Innes, D. R. Turner, B. Moubaraki, K. S.Murray, Dalton Trans. 39 (2010) 149-159.

[35] M. Koike, K. Murakami, T. Fujinami, K. Nishi, N. Matsumoto, Y. Sunatsuki,Inorg. Chim.Acta 399 (2013) 185-192.

[36] C. Faulmann, K. Jacob, S. Dorbes, S. Lampert, I.Malfant, M.-Liesse Doublet, L.Valade, J. A. Real,Inorg. Chem. 46 (2007)8548−8559.

[37]C. Faulmann, J. Chahine, L.Valade, G.Chastanet, J.-F.Létard, D. de Caro,Eur. J. Inorg. Chem. (2013) 1058−1067.

[38] C.-F.Sheu, S.-M.Chen, G.-H.Lee, Y.-H.Liu, Y.-S.Wen, J.-J.Lee, Y.-C. Chuang, Y. Wang,Eur. J. Inorg. Chem. (2013) 894–901.

[39]P. N. Martinho, A. I. Vicente, S.Realista, M. S. Saraiva, A. I. Melato, P.Brandão, L. P. Ferreira, M. de Deus Carvalho,J.Organomet. Chem. 760 (2014) 48-54.

[40] G. -H. Sheng, X. -S. Cheng, Z. -L. You, H. -L. Zhu, Synth. React. Inorg.Met.-Org. Nano-Met. Chem. 45 (2015) 388-391.

[41] S. Naiya, M. G. B. Drew, C. Diaz, J. Ribas, A. Ghosh, Eur. J. Inorg. Chem.(2011) 4993-4999.

[42] R. Biswas, M. G. B. Drew, C. Estarellas, A. Frontera, A. Ghosh, Eur. J. Inorg.Chem. (2011) 2558-2566.

[43] S. Naiya, S. Giri, S. Biswas, M. G. B. Drew, A. Ghosh,Polyhedron 73 (2014) 139-145.

[44] S. -S. Qian, X. Wang, Z. -L. You, H. -L. Zhu, J. Struct.Chem. 55 (2014) 379-383.

[45] P. Pascal, Ann. Phys. Chim. 19 (1910) 5.

[46] P. Pascal, Ann. Phys. Chim. 25(1912)289.

[47] P. Pascal, Ann. Phys. Chim. 28(1913) 218.

[48] G. A. Bain, J. F. Berry, J. Chem. Educ. 85 (2008) 532–536.

[49] *CrysAlisPro*, 2013, Agilent Technologies. Version 1.171.136.128.

[50] R. C. Clark, J. S. Reid, ActaCryst. A51 (1995) 887-897.

[51] L. Palatinus, G. Chapuis, J. Appl. Cryst. 40 (2007) 786-790.

[52] L. Farrugia, J. Appl. Cryst. 45 (2012)849-854.

[53] G. M. Sheldrick, ActaCrystallogr. A64 (2008)112−122.

[54] G. M. Sheldrick, SADABS: Software for Empirical Absorption Correction, University of Gottingen, Institute fur AnorganischeChemiederUniversitat, Gottingen, Germany, 1999-2003.

[55] M. A. Spackman, D. Jayatilaka, CrystEngComm 11 (2009) 19-32.

[56] F. L. Hirshfeld, Theor. Chim. Acta 44 (1977) 129-138.

[57] H. F. Clausen, M. S. Chevallier, M. A. Spackman, B. B. Iversen, New J. Chem. 34 (2010) 193-199.

[58] A. L. Rohl,. M. Moret, W. Kaminsky, K. Claborn, J. J. McKinnon, B. Kahr, Cryst. Growth Des. 8 (2008) 4517-4525.

[59] A. Parkin, G. Barr, W. Dong, C. J. Gilmore, D. Jayatilaka, J. J. McKinnon, M. A. Spackman, C. C. Wilson, CrystEngComm9 (2007) 648-652.

[60] M. A. Spackman, J. J. McKinnon, CrystEngComm 4 (2002) 378-392.

[61] S. K. Wolff, D. J. Grimwood, J. J. McKinnon, D. Jayatilaka, M. A. Spackman, Crystal Explorer 2.0; University of Western Australia: Perth, Australia, 2007. http://hirshfeldsurfacenet.blogspot.com/.

[62] F. H. Allen, O. Kennard, D. G. Watson, L. Brammer, A. G. Orpen, R. J. Taylor, J. Chem. Soc., Perkin Trans. 2 (1987) S1-S19.

[63] J. J. Kinnon, M. A. Spackman, A. S. Mitchell, Acta Crystallogr. B60 (2004) 627-668.

[64] A. Bhattacharyya, P. K. Bhaumik, P. P. Jana, S. Chattopadhyay, Polyhedron 78 (2014) 40-45.

[65] S. Jana, S. Chatterjee, S. Chattopadhyay, Polyhedron 48 (2012) 189–198.

[66] P. K. Bhaumik, S. Jana, S. Chattopadhyay, InorganicaChimica Acta 390 (2012) 167–177.

[67] L. Chen, W. Zhang, S. Huang, X. Jin, W.-H. Sun, Inorg. Chem. Commun. 8 (2005) 41-43.

[68] H. Furutachi, A. Ishida, H. Miyasaka, N. Fukita, M. Ohba, H. Okawa, M. Koikawa, J. Chem. Soc., Dalton Trans. (1999) 367-372.

[69] I. Nemec, R. Herchel, Z. Trávnícek, Dalton Trans. 44 (2015) 4474–4484.

[70] F. Yu, Y.-M. Zhang, A.-H.Li, B. Li,Inorg. Chem. Commun. 51 (2015) 87–89.

[71] A. B. Gaspar, M. Seredyuk, Coord. Chem. Rev. 268 (2014) 41–58.

[72] O. Khan, Molecular Magnetism, VCH Publisher, Inc., New York, USA, 1993, 23.

[73] F.E. Mabbs, D.J. Machin,Magnetism and Transition Metal Complexes, Chapman and Hall, London, 1973.

[74] M. Gómez-Gallego, I. Fernández, D. Pellico, A. Gutiérrez, M. A. Sierra,J. J. Lucena, Inorg. Chem. 45 (2006) 5321–5327.

[75] M. Koike, K. Murakami, T. Fujinami, K.Nishi, N. Matsumoto, Y. Sunatsuki, Inorg. Chim.Acta 399 (2013) 185–192.

[76] S. Alvarez, J. Cirera, Angew. Chem. Int. Ed. 45 (2006) 3012–3020.

[77] M. F. Bush, J. T. O'Brien, J. S. Prell, R. J. Saykally, E. R. Williams, J. Am. Chem. Soc. 129 (2007) 1612-1622.

[78] F. A. Cotton, S. Herrero, R. Jiménez-Aparicio,C. A. Murillo, F. A. Urbanos, D. Villagrán, X. Wang, J. Am. Chem. Soc. 129 (2007) 12666-12667.

[79] M. A. Spackman, P. G. Byrom, Chem. Phys. Lett. 267 (1997) 215-220.

Table 1: Crystal data and refinement details of complexes **1**and **2**

Complex	**1**	**2**
Formula	$C_{24}H_{38}Br_2ClFeN_{10}O_8$	$C_{30}H_{44}ClFeN_6O_9S_2$
Formula Weight	845.73	788.13
Temperature (K)	173	273
Crystal system	Monoclinic	Orthorhombic
Space group	*C2/c*	*Pnma*
a(Å)	12.67(3)	9.9232(3)
b(Å)	9.14(2)	28.5197(10)
c(Å)	28.99(6)	13.5489(5)
β(deg)	96.58(2)	(90)
Z	4	4
d_{calc} (g cm-3)	1.685	1.365
μ (mm-1)	2.990	0.627
F(000)	1716	1652
Total Reflections	6439	47187
Unique Reflections	2941	3315
Observed data [I > 2 σ	2615	2280
No. of parameters	219	247
R(int)	0.020	0.070
R1, wR2 (all data)	0.0387, 0.0971	0.0903, 0.1979
R1, wR2 [I > 2 σ (I)]	0.0445, 0.0927	0.0609, 0.1737

Table 2: Selected bond lengths (Å) and bond angles (°) for complexes **1** and **2**

Complex	**1**	**2**
Fe(1)-O(1)	1.933(2)	1.948(3)
Fe(1)-N(1)	2.136(3)	2.115(3)
Fe(1)-N(3)	2.086(4)	2.082(4)
O(1)-Fe(1)-N(1)	88.08(1)	91.31(1)
O(1)-Fe(1)-N(3)	99.66(1)	89.47(1)
N(1)-Fe(1)-N(3)	90.05(1)	91.16(1)

Table 3: Hydrogen bond distances (Å) and angles (º) for complexes **1** and **2**.

Complex	D–H···A	D–H	D···A	H···A	∠ D–H···A	Symmetry transformation
1	N(2)-H(2A)···O(2)	1.00	2.758(6)	1.77	171.00	1/2+x,1-y,z
	O(2)-H(2B)···O(1)	0.87	3.078(5)	2.49	125.00	1/2-x,3/2-y,1/2-z
	O(2)-H(2C)···N(3)	0.87	2.92(5)	2.09	158.00	1/2-x,3/2-y,1/2-z
2	N(2)-H(2A)···O(2)	0.98	2.848(5)	1.88	169.00	1-x,1-y,1-z

D, donor; H, hydrogen; A, acceptor

Table 4: Geometric features of the C–H···π interactions of complexes **1** and **2.**

Complex	C–H····Cg(Ring)	H····Cg (Å)	C–H····Cg (°)	C····Cg (Å)	Symmetry transformation
1	C(10)–H(10B)···Cg(3)	2.92	139	3.723(4)	1-x,1/2+y,1/2-z
	C(12)–H(12A)···Cg(3)	2.95	113	3.456(7)	1-x,-1/2+y,1/2-z
2	C(15)–H(15B)···Cg(3)	2.88	123	3.502(6)	1/2+x,y,1/2-z

For complex **1,** Cg(3) = Centre of gravity of 6-membered ring [C(1)–C(2)–C(3)–C(4)–C(5)–C(6)]**;**For complex **2,** Cg(3) = Centre of gravity of 6-membered ring [C(2)–C(3)–C(4)–C(5)–C(6)–C(7)].

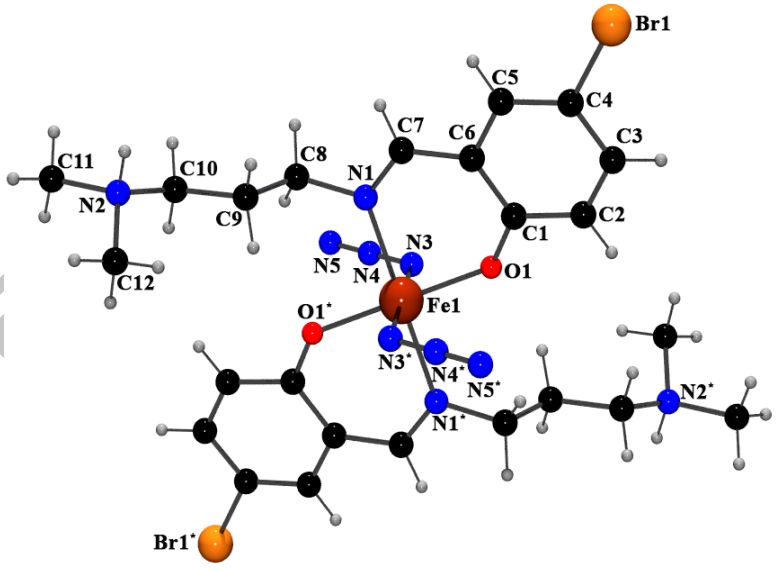

Figure 1: Perspective view of complex **1** with selective atom numbering scheme. perchlorate ion and solvent water molecules are not shown for clarity.

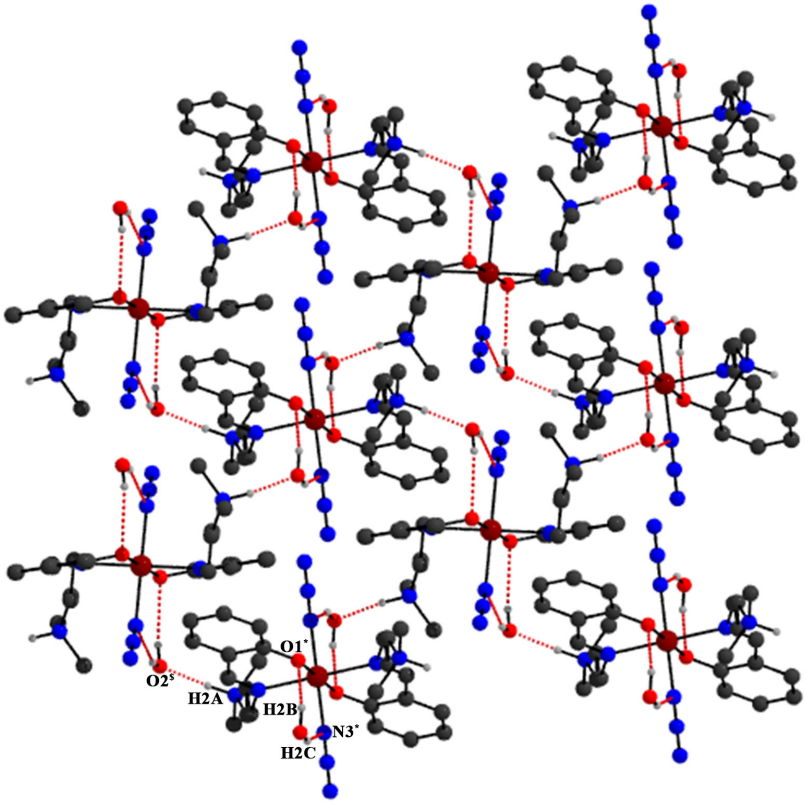

Figure 2: Two dimensional hydrogen bonded architecture of complex **1**. Hydrogen bonds are shown by red dotted lines. Only relevant atoms are shown.

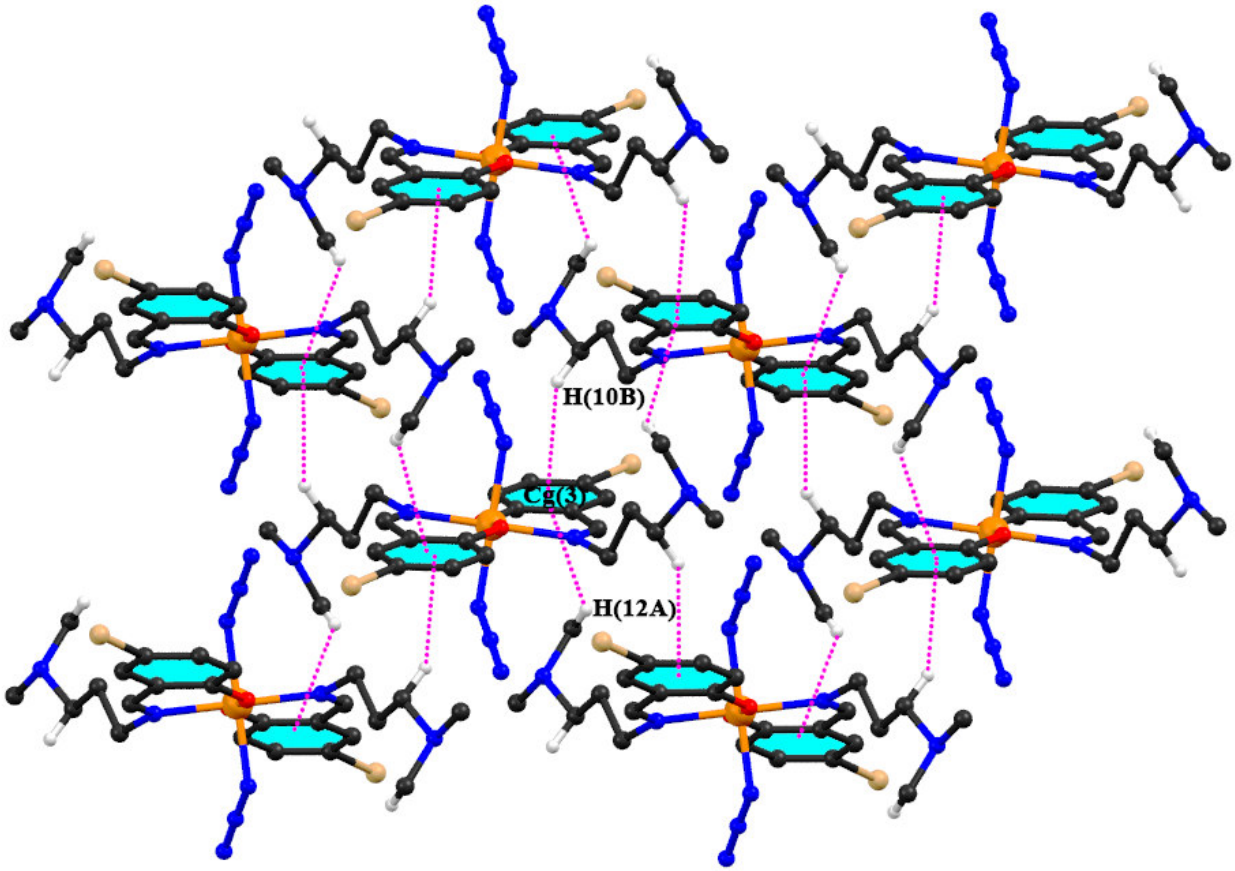

Figure 3: Two dimensional supramolecular architecture of complex **1** via C–H···π interactions**.** Only relevant atoms are shown.

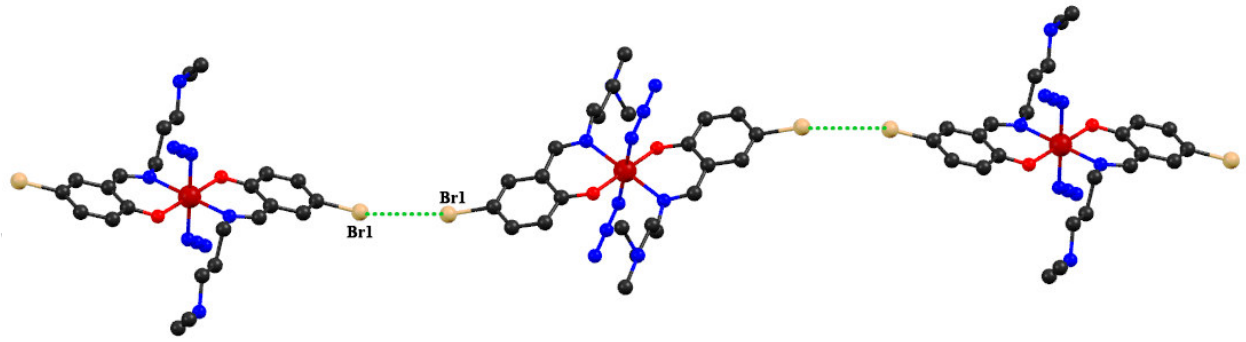

Figure 4: One dimensional chain of complex **1** via Br···Br interactions along crystallographic a axis.

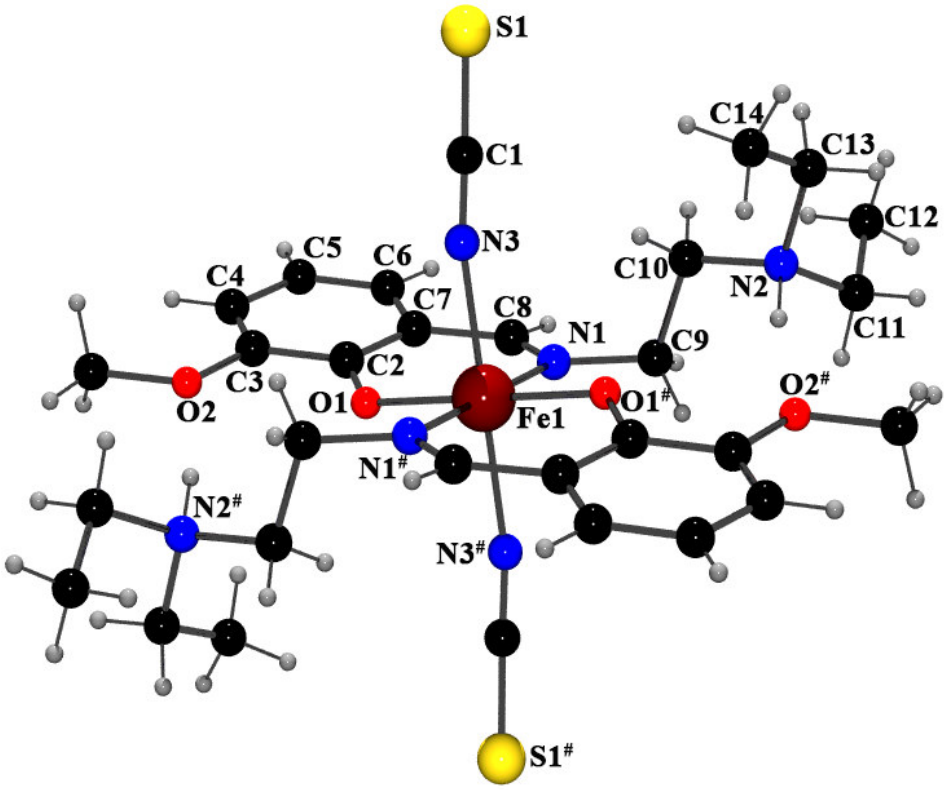

Figure 5: Perspective view of complex **2** with selective atom numbering scheme. Hydrogen bonds are shown by red dotted lines. Solvent water molecule and perchlorate ion are not shown for clarity.

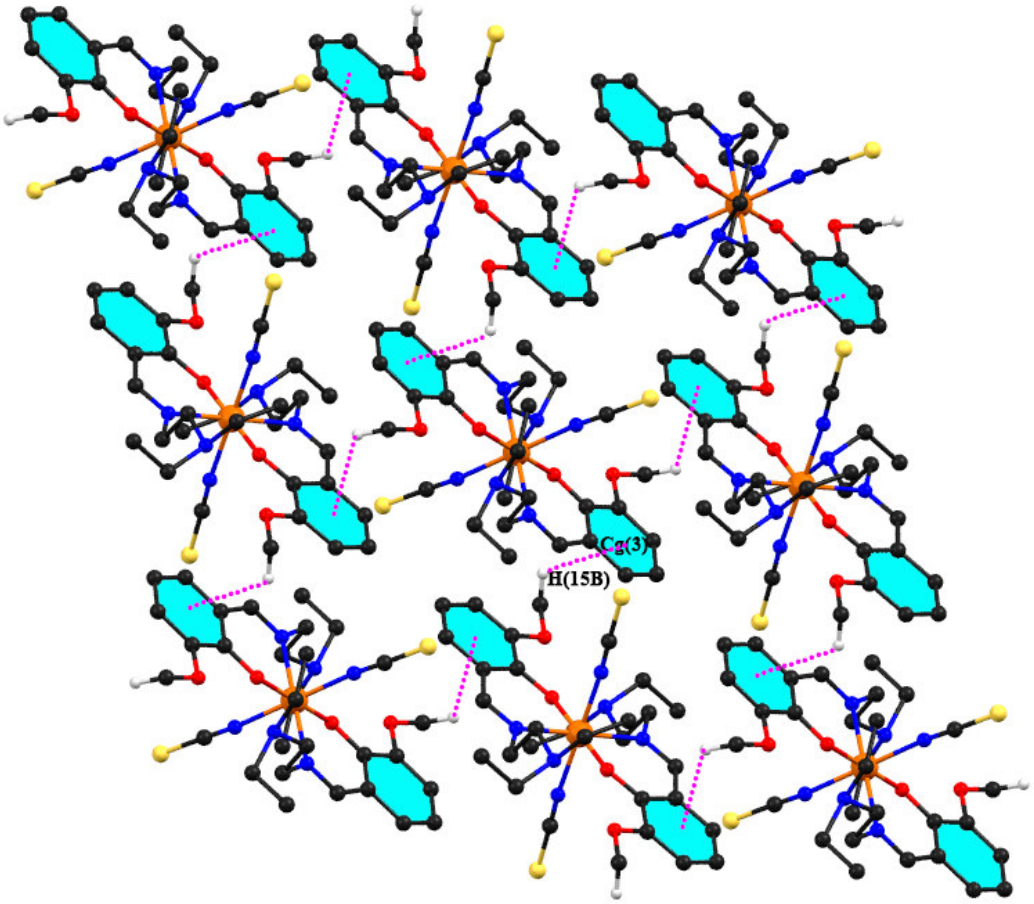

Figure 6: Two-dimensional supramolecular sheet of complex **2** via C–H···π interactions**.** Only relevant atoms are shown.

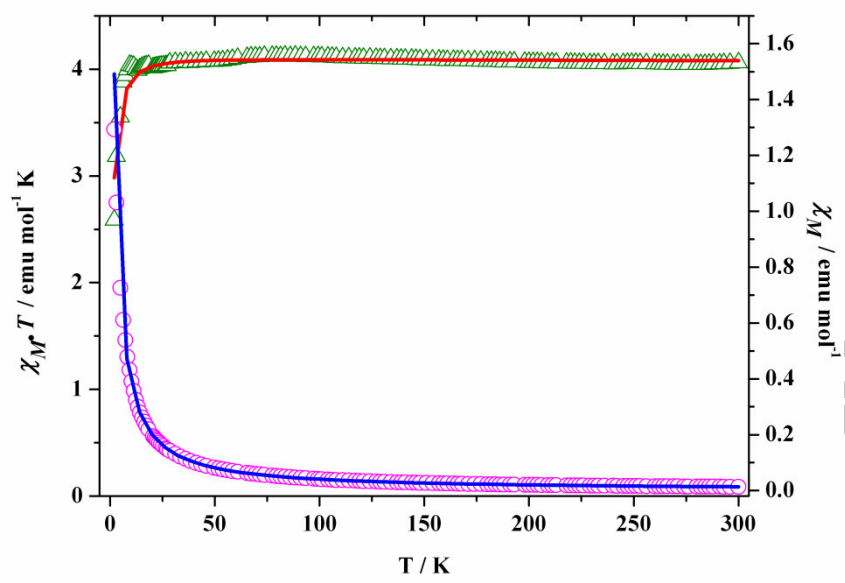

Figure 7: Plot of magnetic susceptibility (○) and $\chi_M \cdot T$ (Δ) *vs* T for complex **2**. The solid lines are the result of fitting the experimental data with Eq. 1.

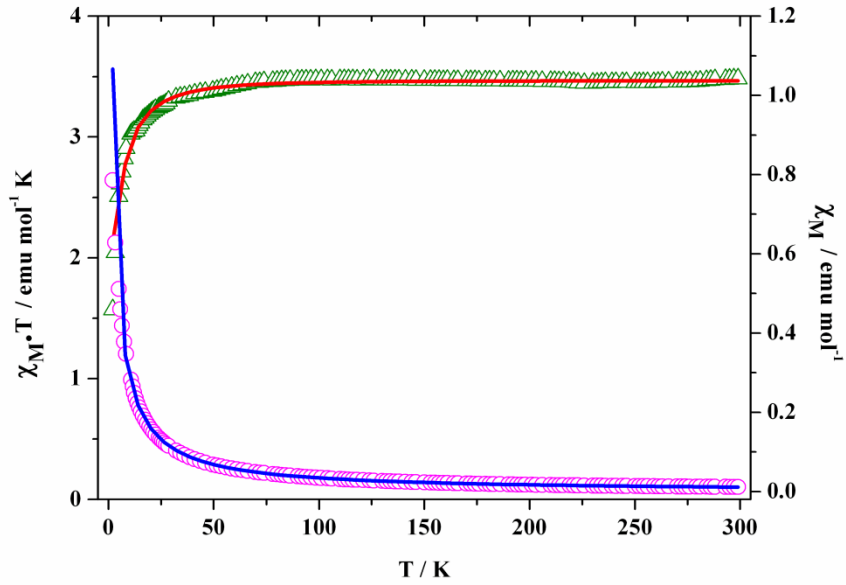

Figure 8: Plot of magnetic susceptibility (○) and $\chi_M \cdot T$(Δ) *vs* T for complex **1**. The solid lines are the result of fitting the experimental data with Eq. 2.

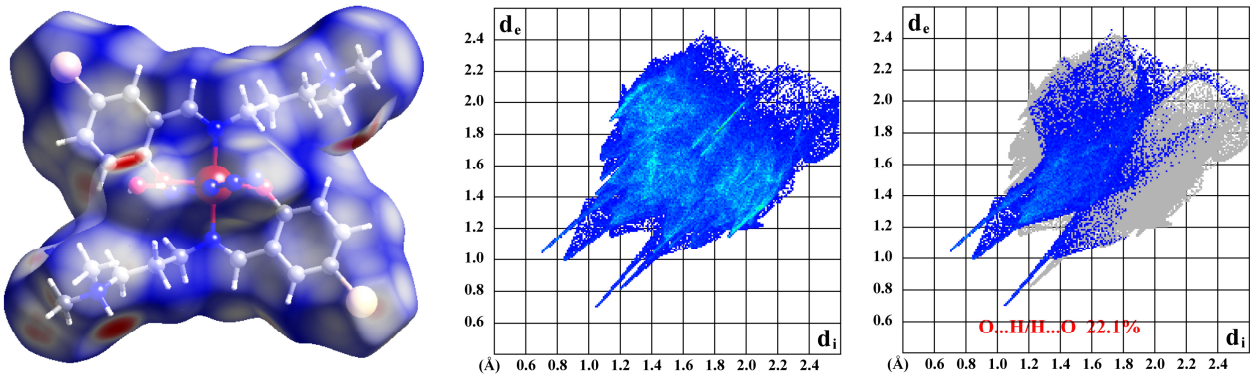

(a) (b) (c)

Figure 9: (a) Hirshfeld surface mapped over d_{norm}. (b) two dimensional fingerprint plots. (c) two dimensional fingerprint plots with the O···H/H···O interactions highlighted in colour for complex **1**.

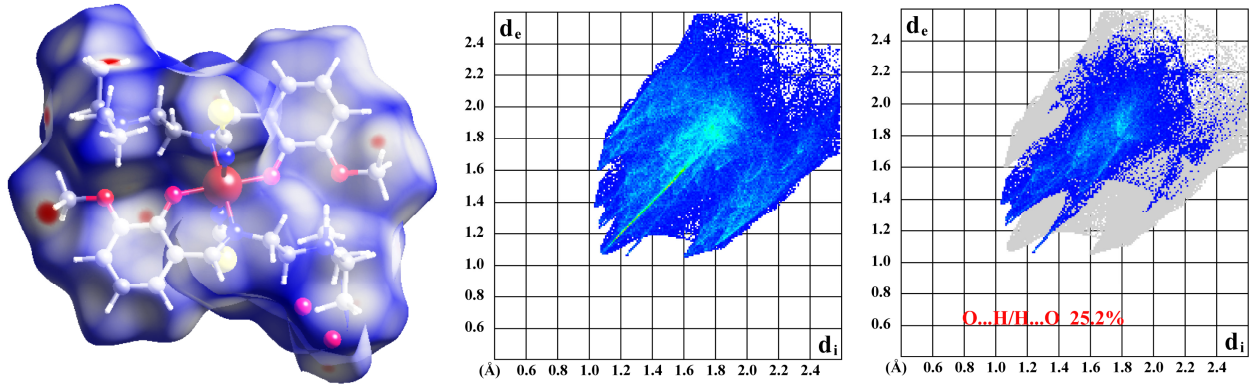

(a) (b) (c)

Figure 10: (a) Hirshfeld surface mapped over d_{norm}. (b) two dimensional fingerprint plots. (c) two dimensional fingerprint plots with the O···H/H···O interactions highlighted in colour for complex **2**.

Synthesis, characterization and magnetic study of two new octahedral iron(III) complexes with pendant zwitterionic Schiff bases

Subrata Jana, Anik Bhattacharyya, Biswa Nath Ghosh, Kari Rissanen, Santiago Herrero, Reyes Jiménez-Aparicio, Shouvik Chattopadhyay

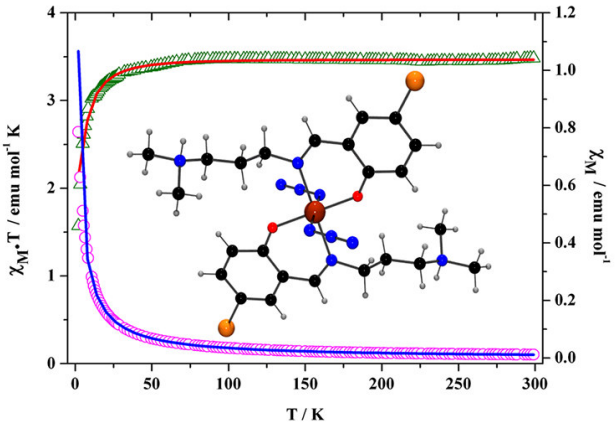

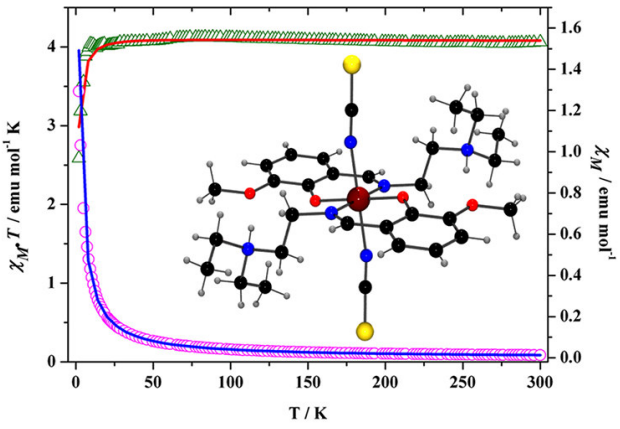

Synthesis, characterization and magnetic study of two new octahedral iron(III) complexes with pendant zwitterionic Schiff bases

Subrata Jana, Anik Bhattacharyya, Biswa Nath Ghosh, Kari Rissanen, Santiago Herrero, Reyes Jiménez-Aparicio, Shouvik Chattopadhyay

Two new octahedral iron(III) complexes have been synthesized. Single crystal X-ray diffraction studies confirm their structures. In both complexes, Schiff bases are trapped in their zwitterionic forms and behave as bi-dentate ligands, keeping the remaining potential donor sites pendant. Variable temperature magnetic susceptibilities were measured and no evidence of spin crossover could be observed.

Synthesis, characterization and magnetic study of two new octahedral iron(III) complexes with pendant zwitterionic Schiff bases

Subrata Jana, Anik Bhattacharyya, BiswaNath Ghosh, Kari Rissanen, Santiago Herrero, Reyes Jiménez-Aparicio, Shouvik Chattopadhyay

Research Highlights

- Synthesis and characterization of two new octahedral iron(III) complexes
- Zwitterionic Schiff bases behaving as pendant ligands
- Molecular structures on the basis of X-ray crystallography
- Measurement of variable temperature magnetic susceptibilities